

1 **Role of Seasonal Importation and Random Genetic Drift on Selection for Drug-**  
2 **Resistant Genotypes of *Plasmodium falciparum* in High Transmission Settings**

3 Robert J. Zupko [0000-0001-8757-483X]<sup>1\*</sup>, Joseph L. Servadio [0000-0002-9988-5712]<sup>1</sup>, Tran Dang  
4 Nguyen [0000-0002-5118-8432]<sup>1</sup>, Thu Nguyen-Anh Tran [0000-0001-6789-5900]<sup>1</sup>, Kien Trung Tran  
5 [0000-0003-3046-8547]<sup>1</sup>, Anyirékun Fabrice Somé [0000-0002-1530-1493]<sup>2</sup>, Maciej F. Boni [0000-0002-  
6 0830-9630]<sup>1,3</sup>

7

8 <sup>1</sup> Center for Infectious Disease Dynamics, Department of Biology, Pennsylvania State University,  
9 University Park, PA, USA

10 <sup>2</sup> Institut de Recherche en Sciences de la Santé, Direction Régionale de l'Ouest, Bobo Dioulasso, Burkina  
11 Faso

12 <sup>3</sup> Nuffield Department of Medicine, University of Oxford, Oxford, UK

13 \* Corresponding Author: [rbz5100@psu.edu](mailto:rbz5100@psu.edu)

14

15 Subject Areas: Anti-Malaria Drug Resistance, Burkina Faso, Malaria, Importation, Genetic Drift

16

17

18 Date of this Draft: October 13, 2023 (7982 words)

19

20 **Abstract**

21 Historically *Plasmodium falciparum* has followed a pattern of drug resistance first appearing in low  
22 transmission settings before spreading to high transmission settings. Several features of low-transmission  
23 regions are hypothesized as explanations: higher chance of symptoms and treatment seeking, better  
24 treatment access, less within-host competition among clones, and lower rates of recombination. Here, we  
25 test whether importation of drug-resistant parasites is more likely to lead to successful emergence and  
26 establishment in low-transmission or high-transmission periods of the same epidemiological setting, using  
27 a spatial, individual-based stochastic model of malaria and drug-resistance evolution calibrated for Burkina  
28 Faso. Upon controlling for the timing of importation of drug-resistant genotypes and examination of key  
29 model variables, we found that drug-resistant genotypes imported during the low transmission season were,  
30 (1) more susceptible to stochastic extinction due to the action of random genetic drift, and (2) more likely  
31 to lead to establishment of drug resistance when parasites are able to survive early stochastic loss due to  
32 drift. This implies that rare importation events are more likely to lead to establishment if they occur during  
33 a high-transmission season, but that constant importation (e.g., neighboring countries with high levels of  
34 resistance) may produce a greater risk during low-transmission periods.

35

## 36 Introduction

37 Despite recent advances in malaria control resulting in a reduction of prevalence, *Plasmodium falciparum*  
38 malaria continues to be a major public health concern. The widespread use of artemisinin-based  
39 combination therapies (ACTs) has contributed to this reduction in prevalence, but increased usage of ACTs  
40 also increases the selective pressure on the parasites to develop drug resistance. Historically, the emergence  
41 of drug resistance has followed a pattern of first appearing in low transmission settings, such as Southeast  
42 Asia and South America, followed by later migration to high transmission settings. This was the case for  
43 chloroquine and sulfadoxine-pyrimethamine resistant *P. falciparum* [1–4], and more recently, artemisinin-  
44 resistant *P. falciparum* phenotypes which were identified in western Cambodia in 2007-2008 [5,6]. Since  
45 the identification of resistance-associated *kelch13* point mutations [5], artemisinin resistance has been  
46 identified in other parts of Southeast Asia [7,8], Guyana [9,10], Rwanda [11,12], and Uganda [13–15].  
47 Thus, developing a mechanistic understanding as to the cause of delayed emergence or slower evolution of  
48 drug resistance in high-transmission settings is particularly germane in the African context where a  
49 reservoir of *kelch13* mutations currently exists and has the potential for rapid expansion [16].

50 Several mechanisms have been proposed to explain this pattern of slower drug-resistance emergence,  
51 establishment, and/or evolution in higher transmission regions. First, due to higher population-level  
52 immunity to malaria, a new infectious mosquito bite is less likely to lead to malaria symptoms in a higher  
53 transmission region, resulting in a lower probability that a new infection will be treated by drugs [17–19].  
54 Second, treatment coverage and access are generally lower in high-transmission regions, meaning that new  
55 symptomatic infections will also have a lower chance of facing treatment. Third, multiclonal infections  
56 (i.e., infections in which the host is infected with several genetically distinct strains of the parasite) result  
57 in within-host competition which may suppress drug-resistant clones due to their cost of resistance or  
58 immune-mediated competition [20–23]. Within high transmission settings, such as sub-Saharan Africa,  
59 multiclonal infections are common [24], thus creating the relevant conditions for drug-resistant and drug-  
60 sensitive parasites to be present in the same host. A counteracting factor of this mechanism is that in the  
61 presence of the relevant drug therapy, the demise of drug-sensitive parasites in a multiclonal infection may  
62 result in competitive release of the drug-resistant parasite and accelerate its spread [21]. Finally, higher  
63 rates of recombination in high transmission regions may act against multigenic drug-resistant genotypes by  
64 breaking up beneficial combinations of drug-resistance mutations [25] though much work remains to be  
65 done on this question.

66 A growing body of mathematical models suggests that a combination of within-host competition and  
67 immune-mediated symptomology are contributors to the cause of the delayed drug resistance emergence in  
68 high transmission settings [18,20,21,26–31]. Of particular note is the work of Bushman et al. [21] who used

69 an individual-based model (IBM) combined with ordinary differential equations to model within-host red  
70 blood cells, immune response, and parasite dynamics to explore the role of within-host competition. The  
71 study found that resistant genotypes initially have a higher risk of extinction in high transmission settings,  
72 but resistance can rapidly spread if extinction is avoided. These findings are supported by Whitlock et al.  
73 [20] using a similar IBM approach; however, their model also accounted for variations in the antigenic  
74 response to various strains of the parasite. Similarly, Masserey et al. [31] also used an IBM coupled with  
75 an emulator based approach to examine the impact that various factors such as drug  
76 pharmacokinetics/pharmacodynamics, treatment coverage, parasite biology, and environmental factors  
77 have on the establishment of drug resistance.

78 Despite the complexity of the models that have been developed, the effects of spatial-temporal diversity  
79 on *P. falciparum* evolution has not been fully explored [32], and it is unknown in which epidemiological  
80 scenarios importation of drug-resistant parasites presents the most risk – a question that we explore here.  
81 In the context of the high-transmission regions of sub-Saharan Africa, the malaria burden is not uniformly  
82 distributed [33], and a country may contain regions of high and low transmission which may influence the  
83 evolutionary environment for resistant genotypes. Another limitation of prior studies is that even high  
84 transmission regions can have significant seasonal variation in transmission patterns with periods of  
85 comparatively low transmission occurring outside of the peak transmission season. Accordingly, there has  
86 been increasing interest in the role that seasonality plays in malaria transmission, with recent studies  
87 suggesting that persistent asymptomatic infections allow for dry season survival [34]. Finally, while  
88 importation is a known mechanism through which drug-resistance has been introduced into various  
89 countries, the actual risk of establishment or fixation post-importation is unknown. A contributing factor is  
90 the inherent complication in surveillance efforts to monitor importation. While data are limited, in a  
91 retrospective study of 54 international travelers arriving in Italy from 2014 to 2015 with confirmed cases  
92 of *P. falciparum* malaria, 9 genetic markers for drug resistant genotypes were detected, suggesting that the  
93 rate of importation across national borders may be substantial [35], a finding echoed by an earlier study  
94 [36].

95 In this study we explore a straightforward importation mechanism for the introduction of drug  
96 resistance in high-transmission regions, through the application of a spatial, IBM of malaria that was  
97 previously calibrated and validated for Burkina Faso [37]. This simulation also allows us to explore the role  
98 of seasonality and how importation of drug-resistant parasites may lead to the emergence and establishment  
99 of drug resistance in a realistic high-transmission context with seasonal variation and heterogeneity of  
100 malaria transmission. By restricting importation in the simulation to a particular month, we are able to

101 calculate extinction probabilities and follow long-term trajectories to determine what times of year (and  
102 what importation rates) pose the most risk for the establishment and spread of drug resistance.

103

## 104 **Methods**

105 Here we use the term *appearance* to refer to the period following the importation of one or more  
106 artemisinin-resistant genotypes (called 580Y for short, using the most common allele found so far). Not all  
107 importations are successful, and an imported genotype may immediately go extinct (i.e., no further  
108 transmission), or have a brief period of transmission before going extinct. If the genotype is able to survive  
109 the action of random genetic drift surrounding its appearance, we say that it has *successfully emerged* once  
110 its allele frequency is greater than 0.001 ( $10^{-3}$ ) allowing for possible progression to fixation as the dominant  
111 strain [38].

112

### 113 *Simulation Overview*

114 We utilized a previously calibrated and validated spatial IBM of malaria and human movement in Burkina  
115 Faso [37,39,40]. As the simulation was designed and constructed with the intent of exploring the evolution  
116 of drug resistance in *P. falciparum* [39], it has the appropriate components necessary to explore the  
117 mechanisms for delayed emergence without being constructed explicitly for it. The simulation models  
118 Burkina Faso as a grid of 10,936 5km-by-5km cells (approximately 273,400 km<sup>2</sup>) and uses an initial  
119 population of 3.6 million individuals (25% of the 2007 population) (Supplemental Material 1, §2 – 4).  
120 Malaria transmission follows the holoendemic patterns of Burkina Faso with the median  $PfPR_{2-10}$  in a given  
121 cell ranging between 7.9% to 67.6% [41]. Transmission also follows a seasonal pattern, with transmission  
122 increasing at the start of the rainy season in late-May to early-June, peaking between August to October,  
123 and declining to a seasonal low in November [37]. On a regional level, the transmission season may be  
124 shorter or longer depending upon the length of the rainy season, with the northern Sahelian climatic region  
125 having a heightened transmission of about three months, while the season lasts for about five months in the  
126 southern Sudanian climatic region.

127 Upon model initialization, the simulated landscape initially consists of parasites that are chloroquine  
128 resistant, artemisinin and piperazine sensitive, and either amodiaquine sensitive or resistant with a 50-50  
129 probability. Following model burn-in, mutation by the parasite in the presence of the relevant therapy is  
130 enabled based upon previously calibrated mutation rates [42], under the assumption that the large majority  
131 of mutation occurs during asexual blood stage replication [43]. When locally transmitted infections occur

132 via new infectious bites, individuals may remain asymptomatic, or progress to clinical symptoms based  
133 upon their individual immune response. Upon presenting with clinical symptoms, individuals seek  
134 treatment following preconfigured rates for Burkina Faso. Individuals under 5 years of age follow  
135 treatment-seeking rates determined by previous Malaria Indicator Survey findings [44], while individuals  
136 over 5 seek treatment at a rate that is 55% (absolute value) of the under-5 rate. This treatment seeking rate  
137 also increases at a rate of 3% starting in model year 2019, consistent with the expected expansion of  
138 treatment seeking by individuals [45]. Treatment seeking does not ensure that an efficacious ACT will be  
139 taken as the private market accounts for 16.8% of treatments in the simulation, consistent with the local  
140 treatment landscape [44].

141 The individual immune response is summarized as follows, with the full scope elucidated in Nguyen et  
142 al. [39] and relevant changes included below. Upon being selected by the simulation to be bitten by an  
143 infectious mosquito, the individual undergoes a sporozoite challenge during which their immune response  
144 may result in sporozoites being cleared before the parasite enters the liver stage [37]. Based upon the  
145 individual's immune response the probability of infection ranges from 20% (high immune response) to 80%  
146 (low immune response). Successful infections proceed to the blood stage where the total parasitemia  $D_R$ ,  
147 where  $R$  notes the specific *P. falciparum* clone, is initially set based upon a random uniform draw from the  
148 appropriate parasitemia range (e.g., clinical infections will draw from a range of  $10^{10}$  to  $10^{12}$  parasites per  
149 microliter of blood).

150 Clearance of the parasite by the immune system is then based upon the following calculation:

$$D_{R,t+K} = (1 - C_R)(0.8036 \cdot (1 - M_t) + 0.9572 \cdot M_t)^K \quad (1)$$

151  
152 Where  $D_{R,t}$  represents the parasite density at time  $t$ ,  $M_t$  represents the host immune response using a scale  
153 from zero to one, and  $C_R$  represents the fitness cost of the given strain with zero representing the wildtype  
154 (i.e., no fitness cost). The parasite density is updated asynchronously every seven days ( $K = 7$ ) and prior  
155 validation ensured that this did not differ from daily updating and informed the numeric values used in the  
156 equation [39]. In the event of a new infection (resulting in a multiclonal infection), or clearance of a prior  
157 infection, the parasite density is updated prior to the next scheduled seven-day update interval.

158 As individuals are infected and clear infections, the individual immune response; described by the  
159 variable  $\Theta$ ; increases according to rates parameterized in Nguyen et al. [39], and impacts the probability  
160 that any new infection will progress to clinical symptoms as follows:

$$Pr_{clin} = \frac{0.99}{1 + \left(\frac{\theta}{\theta_{mid}}\right)^z} \quad (2)$$

161  
162 where  $\theta_{mid}$  describes the point at which immunity confers a 50% chance of developing symptoms, and  $z$   
163 describes the relationship between the level of immunity and the likelihood of developing symptoms [46].  
164 If individuals go an extended period of time without exposure,  $\theta$  decays with a half-life of 400 days,  
165 resulting in an increasing likelihood that an individual will experience malaria symptoms following a new  
166 infectious mosquito bite.

167 Individuals are infected in the population based upon the force of infection (FOI) of parasites present  
168 in a given cell, with individual host parasitemia used to calculate the FOI of *P. falciparum* clone  $R$ , at time  
169  $t$ , for all hosts  $n$  such that:

$$D_i = \sum_{j=1}^{c_i} \delta_{j,i} \gamma_{j,i} \quad (3)$$

$$\Lambda_{t,R} = \beta \sum_{i=1}^n g(D_i) \cdot b_i \cdot D_{R,t+K} \quad (4)$$

170  
171 Where Equation 3 describes the total parasitemia  $D_i$  of an individual where the quantity of the parasite  
172 density of clone  $j$  in the host is given by  $\delta_{j,i}$ , with  $\gamma_{j,i}$  representing the presence/absence of gametocyte  
173 production of the clone  $j$  where one represents normal production and zero represents none. Due to the  
174 nature of the simulation, the residual gametocytaemia following a cured infection (i.e., the asexual  
175 parasitemia is zero) is not simulated. To compensate for this the gametocytaemic period is shifted earlier  
176 so that infectious hosts have the same number of infectious days as real infections, and overall, this does  
177 not impact the simulation since gametocytocidal drugs are not included in the simulation.

178 Equation 4 describes the FOI for  $R$  where  $b_i$  is the biting attractiveness of the host, function  $g$  describes  
179 the saturation of transmission probability with increasing parasite density as described by Ross et al. [47],  
180 and  $\beta$  represents a scaling factor used to calibrate the entomological inoculation rate for the given location  
181 within the simulation. Thus,  $\Lambda_{t,R}$  is ultimately dependent upon the parasitemia of  $R$  in individuals, resulting  
182 in a link to individual immune response and any fitness cost associated with a given parasite. As a result, a  
183 high fitness cost incurred by drug resistant strains will result in a discounting of the FOI, consistent with  
184 the competitive advantage of the wild type in absence of drug pressure [48,49].

185

## 186 *Study Parameterizations*

187 Using the previously prepared parameterization of Burkina Faso calibrated to the epidemiological situation  
188 as of 2017 [37]. While prevalence and case numbers in Burkina Faso are likely to have changed somewhat  
189 since 2017, the intent of this study is to explore the general behavior of imported parasites and not exact  
190 forecasts of allele frequency. Using this calibration, two simulation studies were conducted, a  
191 comprehensive national scale simulation, and a smaller limited locality study. For the first study, the role  
192 of seasonality on importation was examined by controlling the month of importation, number of importation  
193 events per month (i.e., 1, 3, 6, or 9), and parasite density of the imported infection (i.e., a symptomatic or  
194 asymptomatic infection), yielding a total of 96 combinations. During the month of importation, an  
195 importation may occur on any day, with the exact number of imports on a given day determined using a  
196 Poisson distribution across the entire month. The location of importation is determined by a weighted draw  
197 across the entire population, based upon the total population in each cell within the simulation  
198 (Supplemental Material 1, §5). Due to the population distribution of Burkina Faso having a lower  
199 population in the Sahelian climate zone, this has the effect of biasing importations towards the more densely  
200 populated Sudano-Sahelian (containing Ouagadougou, the capital of Burkina Faso) and Sudanian  
201 (containing Bobo-Dioulasso, the second largest city in Burkina Faso) climate zones (Supplemental Material  
202 1, §3 – 4.

203 Upon selection of a cell, the individual to be infected at the location is determined by a uniform random  
204 draw from all susceptible individuals at that location. The individual is then infected by an artemisinin  
205 resistant *P. falciparum* parasite with the *pfkelch13* allele 580Y, and the host parasitemia level is set to the  
206 appropriate value for a symptomatic (between  $10^{10}$  and  $10^{12}$  parasites per microliter of blood) or  
207 asymptomatic (less than 1,000 parasites per microliter of blood) infection. In the event of a symptomatic  
208 infection, the individual may seek treatment on the basis of their age and the regional treatment seeking rate  
209 which ranges from 52.1% to 87.0% for an individual under-5 and 23.4% to 39.1% for an individual over-  
210 5. If an individual seeks treatment, they receive either artemether–lumefantrine (68% of treatments),  
211 amodiaquine (12.4%), quinine (5.6%), dihydroartemisinin-piperaquine (4.9%), artesunate–amodiaquine  
212 (2.5%), artesunate (2.2%), artesunate, sulfadoxine/pyrimethamine (1.6%), chloroquine (1.5%), or  
213 mefloquine (1.3%) with the probability of a specific treatment based upon previous survey data and the  
214 make-up of the nationally recommended first-line therapies and private-market treatments [37,44,50].  
215 Although importation is implemented by importing a singly-infected individual, following importation  
216 multiclonal infections are possible if the individual is infected by another clone. Following model burn-in,



217 the simulation is allowed to run for twenty years. In order to ensure the statistical validity of the results, 50  
218 replicates of each combination were run, for a total of 3,600 replicates.

219 Following evaluation of a drug-resistant genotype establishing under various importation conditions,  
220 additional reporting was incorporated to capture additional population immunity data and three additional  
221 parameterizations were prepared. These changes allowed for an assessment of the mechanisms of delayed  
222 drug resistance or establishment to be evaluated, within the constraints of the mechanisms that are  
223 implemented within the simulation. For the first parameterization, *de novo* mutations were enabled using a  
224 previously determined mutation rate [42] so that the evolution and spread of drug-resistant genotypes could  
225 be observed

226 Finally, additional model validation was conducted to ensure conformity of multiclonal infections and  
227 multiplicity of infections (MOI) to field conditions. Within the simulation, the proportion of multiclonal  
228 infections fluctuates on a seasonal basis, and the ranges are in good agreement with previous studies. A  
229 sentinel site study in Nanoro, Burkina Faso, located in the Sudano-Sahelian climate zone, was conducted  
230 from September 2010 to October 2012 and recorded a mean MOI of 2.732 ( $\pm 0.056$ ) with a range of 1 to 7  
231 parasite genotypes [51], compared to simulation results of  $2.220 \pm 0.455$  (Supplemental Material 1, §1).

232

### 233 *Limited Locality Studies*

234 Following completion of the national scale studies, additional studies were conducted with a limited  
235 population or limited geographic scope intended to isolate or reproduce dynamics observed in the national-  
236 level model results. Specifically, these more limited models were used to explore if observed seasonal  
237 fluctuations in 580Y frequency and treatment seeking behavior could help to explain observed transmission  
238 and infection dynamics. A total of three additional spatial models were prepared, all deriving from the same  
239 configuration used for the national scale model: a single cell with a population of 100,000, a two-by-two  
240 grid with a total population of 300,000 individuals, and a three-by-three grid with a total population of  
241 320,000 individuals. All models are based upon four different configurations in which the five-month  
242 seasonal pattern of the Sudanian zone is enabled or disabled, and treatment seeking is either balanced (i.e.,  
243 50% of under-5, 50% of over-5) or skewed based upon the national upper and lower bounds (i.e., 87% of  
244 under-5, 23.4% of over-5).

245

## 246 *Statistical Analysis*

247 To examine whether the month of case importation is associated with the frequency of parasites with the  
248 580Y allele, we performed a Kruskal-Wallis test to identify whether differences exist across months,  
249 followed by pairwise Wilcoxon rank-sum tests to identify which pairs of months yielded significantly  
250 different frequencies following importation. This was repeated, collapsing months into the high (June –  
251 October) and low (November – May) transmission seasons to compare these two time periods. This was  
252 followed by examining whether different months of importation are associated with a greater probability  
253 of emergence of the 580Y allele, defined by having a frequency  $\geq 0.001$ , we used chi-squared tests for  
254 proportions. An initial, global chi-squared test identified if any months differed, and subsequent pairwise  
255 tests identified months with different probabilities. Within months, we also tested whether symptomatic or  
256 asymptomatic importation was associated with probability of establishment. All p-values lower than  $10^{-4}$   
257 are reported as  $10^{-4}$ .

258 To show alignment among simulated time trends in total infections, treatment administration, immune  
259 response, and frequency of parasites with the 580Y allele, Spearman's correlation coefficients were  
260 calculated following visual inspection. For pairs of variables with oscillating trends that did not have  
261 aligned peaks and troughs, a lag was applied to align the oscillations, providing insight into how one trend  
262 follows another. The use of a lag is appropriate given the inherent delays associated with infection,  
263 presentation of symptoms, and transmission of *P. falciparum* infections. Correlation coefficients were  
264 calculated for the three climatic regions for scenarios consisting of *de novo* mutation, importation during  
265 the low transmission season, and importation during the high transmission season.

266

## 267 **Results**

### 268 *Role of Seasonality on Importation*

269 When varying the month of importation of drug resistance, the number of importations, and the parasitemia  
270 of the imported individual, there is a clear difference between extinction outcomes and sustained  
271 transmission outcomes when comparing low-transmission months to high-transmission months (Figure 1).  
272 In six of the eight combinations for symptomatic/asymptomatic importation and importation count, drug-  
273 resistant genotypes are more likely to establish when imported during low-transmission months ( $p \leq 0.0007$ ,  
274 Wilcoxon-Rank Sum, Supplemental Materials 2, Table S2). In the scenarios of three asymptomatic  
275 importations or one symptomatic importation, future resistance frequencies appear lower for parasites  
276 imported during low-transmission periods (Figure 1), but the differences are not statistically significant

277 ( $p=0.81$  and  $p=0.41$ , respectively) due to the large number of zeros in each set of simulations. This large  
278 number of zeros for configurations with one or three asymptomatic importations, or one symptomatic  
279 importation per month, underlines the influence of extinction and random genetic drift during the  
280 importation process. If an imported parasite is unlikely to be sampled by a mosquito, then low transmission  
281 periods would be associated with lower risk of establishment. This is most easily seen in the extinction  
282 paths in Figure 2 where importation is rare (i.e., one importation event in a given month) and onward  
283 transmission occurs with low probability due to the asymptomatic nature of the imported infections; in  
284 these scenarios, extinction probabilities are higher for parasites imported during the low-transmission  
285 season. However, averaging across all scenarios, pairwise comparisons of months across the low season  
286 and the high season indicate that 580Y allele frequency after ten years is likely to be a median 1.84-fold  
287 higher (IQR: 0.90 – 3.35) if the allele is imported during the low-transmission season (Supplemental  
288 Materials 2, Table S4), indicating that if importation events are common (i.e., several per month) low-  
289 transmission periods are associated with a higher starting frequency and a higher a probability of emergence  
290 or establishment for the recently imported parasite.

291 While any imported parasite has a small chance of surviving past initial appearance, the likelihood of  
292 progressing to a frequency of  $10^{-3}$ , suggesting emergence has occurred and the parasite is likely to be  
293 observed, in any scenario was generally below 30% (Figure 3). As expected, our analysis shows that a  
294 higher number of importation events is associated with a higher likelihood of eventual establishment  
295 (asymptomatic global  $\chi^2 = 109.3$ ,  $df = 3$ ,  $p < 0.01$ ; symptomatic global  $\chi^2 = 145.9$ ,  $df = 3$ ,  $p < 0.01$ ). Median  
296 probability of progressing past an allele frequency of  $10^{-3}$  is 0.08 (IQR: 0.02 - 0.14; across 56 month-  
297 scenario combinations) when importation occurs during the low-transmission season, and 0.02 (IQR: 0.02  
298 – 0.06; across 40 month-scenario combination) during the high transmission season. These results support  
299 the finding that when a drug-resistant genotype is imported, assuming it can escape the risk of random  
300 extinction, emergence is more probable for imports during the low-transmission season. When importation  
301 is common (9 asymptomatic imports per month, Figure 4), only 2% to 8% of high season importations (i.e.,  
302 between June and October) reach a 580Y allele frequency  $\geq 10^{-3}$ , whereas 4% to 18% of the low season  
303 importations reach a 580Y frequency  $\geq 10^{-3}$ . When the months immediately following the high transmission  
304 season are excluded (i.e., November and December), the range is 12% to 18%, suggesting selection  
305 mechanisms at play during the high transmission season may are still at play for a period of time following  
306 the end of the season.

307

308 *Selection mechanisms during high- and low-transmission seasons*

309 An examination of the short-term changes in malaria dynamics as the transmission season changes suggests  
310 three common effects that may influence the selection strength for drug-resistant genotypes: changes in  
311 drug coverage, changes in symptoms occurrence, and changes in the multi-clonal nature of some infections.  
312 In a seasonal malaria setting, the age distribution of cases can change between low and high season, and if  
313 treatment coverage depends on age, then selection pressure for drug resistance will vary by season as the  
314 total population with clinical infections who seek treatment (i.e., total population treatment coverage) varies  
315 by season. A simple demonstration of this can be seen in a small population model (320,000 individuals  
316 occupying a 3x3 grid) with age-based treatment coverage and seasonal transmission presented as factors in  
317 the analysis. When both seasonality (based upon the five-month Sudanian zone in Burkina Faso) and age-  
318 based treatment coverage (87% coverage for under-5 and 23.4% coverage for over-5) are present then  
319 treatment coverage varies seasonally, in this example between 54% and 60% (Figure 5), in contrast to  
320 constant treatment coverage when seasonality is absent or under equal treatment seeking. The under-5 and  
321 over-5 treatment coverages in this example were chosen as representational of the maxima and minima for  
322 each group based upon provincial coverages. In our national scale simulations of Burkina Faso, population  
323 treatment coverage changes by 2% to 3% (absolute value) between the seasons resulting in weak to  
324 moderate changes in selection pressure (Figure 6).

325 The nature of the simulation allows for the mean level of all individual immune responses to the parasite  
326 to be captured, denoted here as  $\theta_{pop}$ . As expected,  $\theta_{pop}$  follows a lagged seasonal cycle, with  $\theta_{pop}$  having  
327 the strongest Spearman correlation with number of infections three months prior (Figure 6), which is  
328 independent of the number of importations across the six combinations of region and importation timing.  
329 This cycle of  $\theta_{pop}$  increasing and decreasing across seasons creates a linkage between individual immune  
330 responses and the likelihood of symptoms and treatment seeking. However, the  $\theta_{pop}$  value peaks and  
331 troughs between 0.42 and 0.45 (on an immunity scale of zero to one) warranting further investigation as to  
332 whether immunity differences of this magnitude can have an observable effect on selection pressure.

333 One consequence of  $\theta_{pop}$  changing between seasons is that the fraction of malaria parasites currently  
334 residing in symptomatic patients versus asymptomatic patients changes as well. The quantity  $\phi$ , defined as  
335 the ratio of symptomatic infections to all infections [17,19,52] gives a general description of what  
336 proportion of drug-resistant genotypes are currently experiencing positive selection resulting from  
337 treatment and what proportion are currently undergoing negative selection imposed by their fitness cost.  
338 This symptomatic fraction  $\phi$  appears to be generally low, ranging from 0.07 to 0.12, with a higher  
339 proportion of infections subject to drug pressure at the end of the high season than during the middle of the

340 low season. However,  $\varphi$  is out of phase with the treatment coverage suggesting that the net combined effect  
341 of treatment coverage and symptoms presentation may result in negligible changes in evolutionary pressure  
342 during the course of the year (Figure 6).

343 The role of the individual immune response also works in tandem with the role of within-host  
344 competition occurring in multiclonal infections. The high MOI – with a median ranging from 1.747 – 2.268  
345 depending upon the scenario and climatic zone (Supplemental Materials 1, §3) – along with the low  
346 frequency of resistant clones during the appearance and emergence of drug-resistant genotypes indicates  
347 that within-host competition between drug-sensitive and drug-resistant genotypes is likely occurring. The  
348 strength of this effect can be examined within the simulation by comparing the proportion of multiclonal  
349 infections carrying a 580Y clone to all multiclonal infections (Figure 7). This proportion is highest when  
350 median MOI is lowest, towards the end of the high-transmission season, again showing that these seasonal  
351 forces are acting in opposition preventing the formation of a clear picture of when within-host competition  
352 against drug-resistant genotypes should be the strongest.

353

## 354 **Discussion**

355 Drug resistance has always presented a danger to public health goals. For malaria, however, there is time  
356 to prepare as antimalarial drug resistance typically emerges slowly and may take a decade or more to spread  
357 geographically. Here, we look at the effects that importation of drug-resistant genotypes has on the national-  
358 scale malaria epidemiology (modeled here as the high-transmission settings of Burkina Faso) and we ask  
359 whether imported drug-resistant genotypes are more likely to establish if importation occurs in the high-  
360 transmission season or in the low-transmission season. We show that random genetic drift and starting  
361 frequency play an important role in an imported allele's future trajectory, but we are uncertain if change in  
362 selection pressure is substantial enough across transmission seasons to alter a drug-resistant genotype's  
363 evolutionary path after importation.

364 The major evolutionary-epidemiological gap identified in our work is that seasonally changing  
365 selection pressures for drug resistance are not easily identified as such, and that the direction of change may  
366 not always be clear. Three common factors are known to affect drug-resistance evolution across  
367 transmission settings – treatment coverage, symptoms presentation, and within-host competition in multi-  
368 clonal infections – but these factors do not align the same way between seasons in the same epidemiological  
369 setting as they do between countries that have different epidemiological settings. For example, in the  
370 seasonal setting presented here, treatment coverage goes up seasonally at the same time as symptoms  
371 presentation goes down. The proportion of multi-clonal infections harboring at least one drug-resistant

372 genotype is highest when median MOI is lowest, leading to an ambiguous picture or perhaps small  
373 evolutionary differences in terms of when within-host competition may be acting to reduce the frequency  
374 or relative density of drug-resistant genotypes.

375 The traditional population-genetic effects of importation and drift do have their expected behaviors in  
376 our analysis of drug-resistance importation for malaria. Random genetic drift may lead to extinction for  
377 imported mutants with higher probabilities of extinction associated with low importation rates and low  
378 transmission rates. Imported parasites that are not lost due to drift will progress to emergence and  
379 establishment more quickly if the initial importation event occurred in a smaller population, i.e., during  
380 low-transmission season.

381 As in all epidemiological modeling analyses, the model structure itself means that some limitations are  
382 present in the analysis and interpretation. First, the way that symptomatic importations are implemented  
383 may introduce some bias in favor of the parasite. Specifically, (i) immune response is ignored when an  
384 infection is imported and, (ii) treatment seeking behavior is based upon where the individual resides;  
385 however, in practice individuals may be more (or less) likely to seek treatment if symptomatic when passing  
386 through a port of entry. Second, genetic background and age were also not included as factors in the  
387 analysis. Third, this study focused on importation of *pfkelch13* mutants associated with longer clearance  
388 half-lives and high rates of treatment failure, but the treatment failure rate of *pfkelch13* mutants depends  
389 strongly on the presence/absence of certain partner-drug mutations [53,54], as well as the genetic  
390 background that these mutations appeared on. Imported parasites with intrinsically high failure rates would  
391 likely have an easier time avoiding the effects of drift, spreading, and establishing in the population.  
392 Finally, age, as is well known in malaria, is an important factor associated with malaria history and  
393 treatment seeking; and an imported parasites in a younger patients will have different parasitemia levels  
394 and different likelihood of seeking treatment depending on the patient's country of origin, recent history in  
395 high transmission settings, and malaria immunity.

396 The critical public health conversation that this study has implications for is the future of molecular  
397 surveillance for specific *P. falciparum* drug-resistant genotypes that are at risk of being imported from one  
398 country to another. In particular, when transmission is highly seasonal, monitoring for known markers of  
399 drug resistance may be more important during the low-transmission season. This may become increasingly  
400 relevant in the African context with the *de novo* appearance of the drug resistance markers 561H in Rwanda  
401 [11], along with 469Y and 675V in Uganda [14]. In addition to the *de novo* appearance of these markers on  
402 a regional level, at least one instance of the 561H allele has been isolated in Uganda [14,15], suggesting  
403 that cross border migration of drug resistance is already taking place.

404 A major factor for projecting the future evolution of drug resistance is the increased usage of ACTs  
405 within high transmission settings. While the historical pattern has been for the establishment of imported  
406 genotypes following the evolution of drug resistance in low transmission settings, the recent identification  
407 of *de novo* drug resistance in high transmission settings [11,13,16] suggests that low-transmission  
408 appearance may simply be more likely but not a determinative rule for all drug-resistance emergence events.  
409 Given the role that individual immune response plays in creating an environment conducive to the evolution  
410 of drug resistance, understanding the possible impact of upcoming vaccinations (i.e., RTS,S/AS01) on  
411 selection for – or against – drug resistance by the parasites may play a role in speeding up or slowing down  
412 the selection of drug-resistant genotypes [55,56]. Nevertheless, despite some of the known effects of  
413 transmission setting on drug-resistance evolution – via differences in drug coverage and symptoms  
414 presentation, primarily – these effects do not appear to translate to differences between seasons in the same  
415 epidemiological setting. While drift and importation rate do appear to have their traditional effects on the  
416 success of recently imported genotypes into a new population, natural selection on drug resistance does not  
417 appear to be stronger in one part of the malaria season than another, or these selective differences could not  
418 be identified in the Burkina Faso-specific model parameterizations analyzed here.

419

#### 420 **Availability of data and materials**

421 The source code for the base mathematical model and analysis specific to this manuscript can be found on  
422 GitHub at <https://github.com/bonilab/malariaibm-spatial-BurkinaFaso-2022>. Within the repository the  
423 dataset(s) supporting the conclusions of this article (and its additional files) are stored under,  
424 <https://github.com/bonilab/malariaibm-spatial-BurkinaFaso-2022/tree/main/Data>

425

#### 426 **Acknowledgements**

427 Simulations described in this study were performed on the Pennsylvania State University’s Institute for  
428 Computational and Data Sciences’ Roar supercomputer.

429

#### 430 **Funding**

431 This work was supported by National Institutes of Health grants NIAID R01AI153355 (MFB, RJZ, TDN,  
432 TN-AT, KTT) and NIAID F32AI167600 (JLS), and the Bill and Melinda Gates Foundation grants and

433 INV-005517 to Pennsylvania State University (MFB, RJZ, TDN, TN-AT, KTT). The funders had no role  
434 in study design, data collection and analysis, decision to publish, or preparation of the manuscript.

435

## 436 **References**

- 437 1. Wootton JC, Feng X, Ferdig MT, Cooper RA, Mu J, Baruch DI, Magill AJ, Su X. 2002 Genetic  
438 diversity and chloroquine selective sweeps in *Plasmodium falciparum*. *Nature* **418**, 320–323.  
439 (doi:10.1038/nature00813)
- 440 2. Roper Cally, Pearce Richard, Nair Shalini, Sharp Brian, Nosten François, Anderson Tim. 2004  
441 Intercontinental Spread of Pyrimethamine-Resistant Malaria. *Science* **305**, 1124–1124.  
442 (doi:10.1126/science.1098876)
- 443 3. Lynch C, Roper C. 2011 The Transit Phase of Migration: Circulation of Malaria and Its Multidrug-  
444 Resistant Forms in Africa. *PLOS Med.* **8**, e1001040. (doi:10.1371/journal.pmed.1001040)
- 445 4. Packard RM. 2014 The Origins of Antimalarial-Drug Resistance. *N. Engl. J. Med.* **371**, 397–399.  
446 (doi:10.1056/NEJMp1403340)
- 447 5. Ariey F *et al.* 2014 A molecular marker of artemisinin-resistant *Plasmodium falciparum* malaria.  
448 *Nature* **505**, 50–55. (doi:10.1038/nature12876)
- 449 6. Ashley EA *et al.* 2014 Spread of Artemisinin Resistance in *Plasmodium falciparum* Malaria. *N. Engl.*  
450 *J. Med.* **371**, 411–423. (doi:10.1056/NEJMoa1314981)
- 451 7. World Health Organization. 2019 *World Malaria Report 2019*. Geneva: World Health Organization.  
452 See <https://www.who.int/publications/i/item/world-malaria-report-2019>.
- 453 8. Imwong M *et al.* 2020 Molecular epidemiology of resistance to antimalarial drugs in the Greater  
454 Mekong subregion: an observational study. *Lancet Infect. Dis.* **20**, 1470–1480. (doi:10.1016/S1473-  
455 3099(20)30228-0)
- 456 9. Chenet SM *et al.* 2015 Independent Emergence of the *Plasmodium falciparum* Kelch Propeller  
457 Domain Mutant Allele C580Y in Guyana. *J. Infect. Dis.* **213**, 1472–1475. (doi:10.1093/infdis/jiv752)
- 458 10. Mathieu LC *et al.* 2020 Local emergence in Amazonia of *Plasmodium falciparum* k13 C580Y  
459 mutants associated with in vitro artemisinin resistance. *eLife* **9**, e51015. (doi:10.7554/eLife.51015)
- 460 11. Uwimana A *et al.* 2020 Emergence and clonal expansion of in vitro artemisinin-resistant *Plasmodium*  
461 *falciparum* kelch13 R561H mutant parasites in Rwanda. *Nat. Med.* **26**, 1602–1608.  
462 (doi:10.1038/s41591-020-1005-2)
- 463 12. Uwimana A *et al.* 2021 Association of *Plasmodium falciparum* kelch13 R561H genotypes with  
464 delayed parasite clearance in Rwanda: an open-label, single-arm, multicentre, therapeutic efficacy  
465 study. *Lancet Infect. Dis.* **21**, 1120–1128. (doi:10.1016/S1473-3099(21)00142-0)
- 466 13. Balikagala B *et al.* 2021 Evidence of Artemisinin-Resistant Malaria in Africa. *N. Engl. J. Med.* **385**,  
467 1163–1171. (doi:10.1056/NEJMoa2101746)



- 468 14. Asua V *et al.* 2021 Changing Prevalence of Potential Mediators of Aminoquinoline, Antifolate, and  
469 Artemisinin Resistance Across Uganda. *J. Infect. Dis.* **223**, 985–994. (doi:10.1093/infdis/jiaa687)
- 470 15. Conrad MD *et al.* 2023 Evolution of Partial Resistance to Artemisinins in Malaria Parasites in  
471 Uganda. *N. Engl. J. Med.* **389**, 722–732. (doi:10.1056/NEJMoa2211803)
- 472 16. MalariaGEN Plasmodium falciparum Community Project. 2016 Genomic epidemiology of  
473 artemisinin resistant malaria. *eLife* **5**, e08714. (doi:10.7554/eLife.08714)
- 474 17. Lindblade KA, Steinhardt L, Samuels A, Kachur SP, Slutsker L. 2013 The silent threat:  
475 asymptomatic parasitemia and malaria transmission. *Expert Rev. Anti Infect. Ther.* **11**, 623–639.  
476 (doi:10.1586/eri.13.45)
- 477 18. Klein EY, Smith DL, Laxminarayan R, Levin S. 2012 Superinfection and the evolution of resistance  
478 to antimalarial drugs. *Proc. R. Soc. B Biol. Sci.* **279**, 3834–3842. (doi:10.1098/rspb.2012.1064)
- 479 19. Boni MF, Smith DL, Laxminarayan R. 2008 Benefits of using multiple first-line therapies against  
480 malaria. *Proc. Natl. Acad. Sci.* **105**, 14216. (doi:10.1073/pnas.0804628105)
- 481 20. Whitlock AOB, Juliano JJ, Mideo N. 2021 Immune selection suppresses the emergence of drug  
482 resistance in malaria parasites but facilitates its spread. *PLOS Comput. Biol.* **17**, e1008577.  
483 (doi:10.1371/journal.pcbi.1008577)
- 484 21. Bushman M, Antia R, Udhayakumar V, de Roode JC. 2018 Within-host competition can delay  
485 evolution of drug resistance in malaria. *PLOS Biol.* **16**, e2005712.  
486 (doi:10.1371/journal.pbio.2005712)
- 487 22. Hastings IM. 1997 A model for the origins and spread of drug-resistant malaria. *Parasitology* **115**,  
488 133–141. (doi:10.1017/S0031182097001261)
- 489 23. Hastings IM, D’Alessandro U. 2000 Modelling a Predictable Disaster:: The Rise and Spread of Drug-  
490 resistant Malaria. *Parasitol. Today* **16**, 340–347. (doi:10.1016/S0169-4758(00)01707-5)
- 491 24. Touray AO, Mobegi VA, Wamunyokoli F, Herren JK. 2020 Diversity and Multiplicity of P.  
492 falciparum infections among asymptomatic school children in Mbita, Western Kenya. *Sci. Rep.* **10**,  
493 5924. (doi:10.1038/s41598-020-62819-w)
- 494 25. Li EZ, Nguyen TD, Tran TN-A, Zupko RJ, Boni MF. 2022 Assessing emergence risk of double-  
495 resistant and triple-resistant genotypes of *Plasmodium falciparum*. *bioRxiv*,  
496 2022.05.31.494246. (doi:10.1101/2022.05.31.494246)
- 497 26. Legros M, Bonhoeffer S. 2016 A combined within-host and between-hosts modelling framework for  
498 the evolution of resistance to antimalarial drugs. *J. R. Soc. Interface* **13**, 20160148.  
499 (doi:10.1098/rsif.2016.0148)
- 500 27. Cai L, Tuncer N, Martcheva M. 2017 How does within-host dynamics affect population-level  
501 dynamics? Insights from an immuno-epidemiological model of malaria. *Math. Methods Appl. Sci.* **40**,  
502 6424–6450. (doi:10.1002/mma.4466)
- 503 28. Lee TE, Penny MA. 2019 Identifying key factors of the transmission dynamics of drug-resistant  
504 malaria. *J. Theor. Biol.* **462**, 210–220. (doi:10.1016/j.jtbi.2018.10.050)

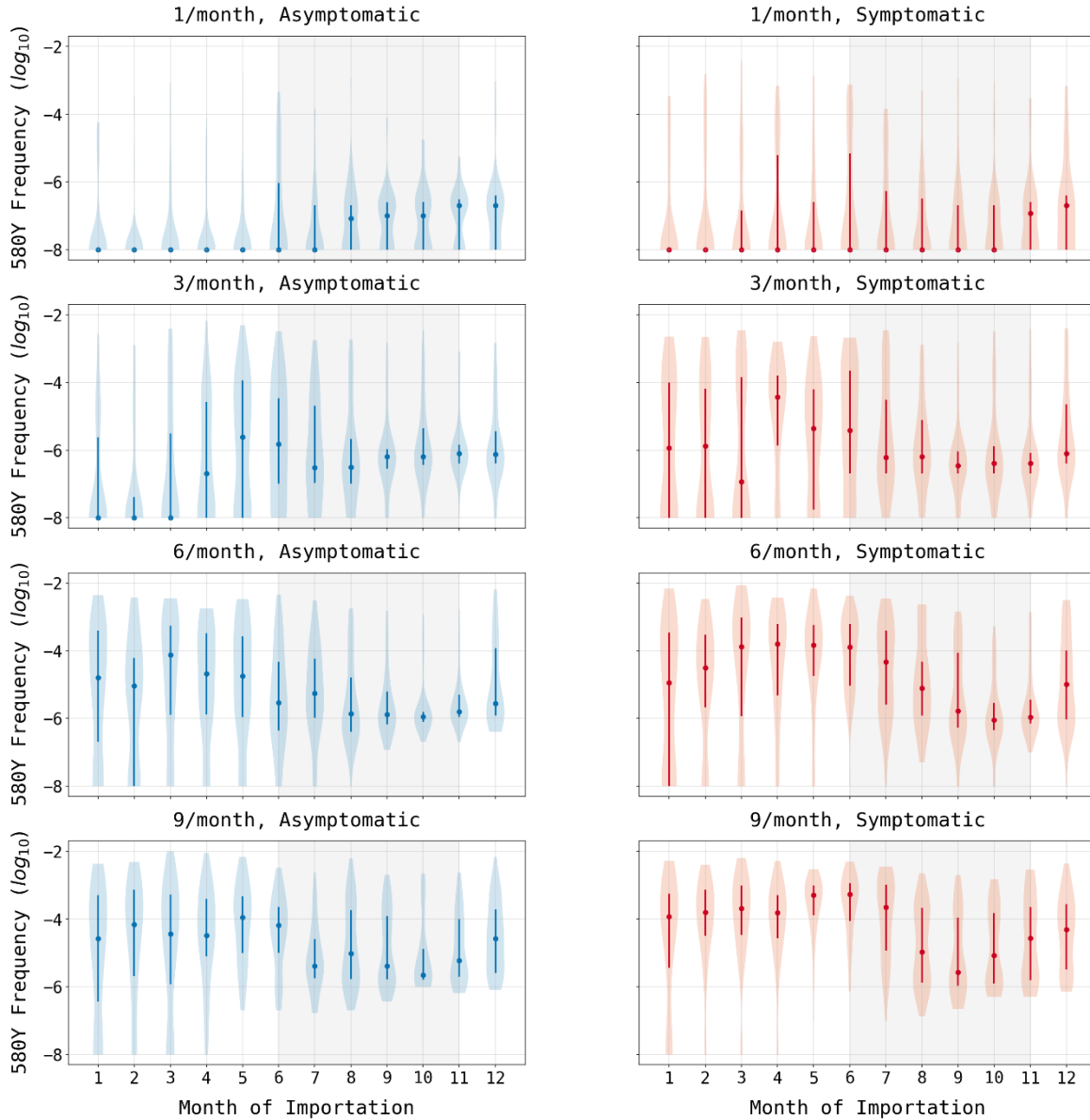
- 505 29. Song T, Wang C, Tian B. 2020 Modelling intra-host competition between malaria parasites strains.  
506 *Comput. Appl. Math.* **39**, 48. (doi:10.1007/s40314-020-1072-5)
- 507 30. Lee TE, Bonhoeffer S, Penny MA. 2022 The competition dynamics of resistant and sensitive  
508 infections. *Results Phys.* **34**, 105181. (doi:10.1016/j.rinp.2022.105181)
- 509 31. Masserey T, Lee T, Golumbeanu M, Shattock AJ, Kelly SL, Hastings IM, Penny MA. 2022 The  
510 influence of biological, epidemiological, and treatment factors on the establishment and spread of  
511 drug-resistant *Plasmodium falciparum*. *eLife* **11**, e77634. (doi:10.7554/eLife.77634)
- 512 32. Sy M *et al.* 2022 *Plasmodium falciparum* genomic surveillance reveals spatial and temporal trends,  
513 association of genetic and physical distance, and household clustering. *Sci. Rep.* **12**, 938.  
514 (doi:10.1038/s41598-021-04572-2)
- 515 33. Ehrlich HY, Jones J, Parikh S. 2020 Molecular surveillance of antimalarial partner drug resistance in  
516 sub-Saharan Africa: a spatial-temporal evidence mapping study. *Lancet Microbe* **1**, e209–e217.  
517 (doi:10.1016/S2666-5247(20)30094-X)
- 518 34. Andrade CM *et al.* 2020 Increased circulation time of *Plasmodium falciparum* underlies persistent  
519 asymptomatic infection in the dry season. *Nat. Med.* **26**, 1929–1940. (doi:10.1038/s41591-020-1084-  
520 0)
- 521 35. L’Episcopia M *et al.* 2021 Artemisinin resistance surveillance in African *Plasmodium falciparum*  
522 isolates from imported malaria cases to Italy. *J. Travel Med.* **28**. (doi:10.1093/jtm/taaa231)
- 523 36. Menegon M, Sannella AR, Severini C, Paglia MG, Matteelli A, Caramello P, Severini F, Taramelli  
524 D, Majori G. 2006 Epidemiologia molecolare della malaria d’importazione in Italia. *Impiego*  
525 *Marcatore Genet. E Saggi Sensib. Vitro Nello Studio Della Clorochino-Resist. Plasmodium*  
526 *Falciparum* **42**, 203–210.
- 527 37. Zupko RJ *et al.* 2022 Long-term effects of increased adoption of artemisinin combination therapies in  
528 Burkina Faso. *PLoS Glob Public Health* **2**, e0000111. (doi:10.1371/journal.pgph.0000111)
- 529 38. Zhao L, Lascoux M, Overall ADJ, Waxman D. 2013 The Characteristic Trajectory of a Fixing Allele:  
530 A Consequence of Fictitious Selection That Arises from Conditioning. *Genetics* **195**, 993.  
531 (doi:10.1534/genetics.113.156059)
- 532 39. Nguyen TD, Olliaro P, Dondorp AM, Baird JK, Lam HM, Farrar J, Thwaites GE, White NJ, Boni  
533 MF. 2015 Optimum population-level use of artemisinin combination therapies: a modelling study.  
534 *Lancet Glob. Health* **3**, e758–e766. (doi:10.1016/S2214-109X(15)00162-X)
- 535 40. Zupko RJ, Nguyen TD, Wesolowski A, Gerardin J, Boni MF. 2023 National-scale simulation of  
536 human movement in a spatially coupled individual-based model of malaria in Burkina Faso. *Sci. Rep.*  
537 **13**, 321. (doi:10.1038/s41598-022-26878-5)
- 538 41. Weiss DJ *et al.* 2019 Mapping the global prevalence, incidence, and mortality of *Plasmodium*  
539 *falciparum*, 2000–17: a spatial and temporal modelling study. *The Lancet* **394**, 322–331.  
540 (doi:10.1016/S0140-6736(19)31097-9)
- 541 42. Watson OJ, Gao B, Nguyen TD, Tran TN-A, Penny MA, Smith DL, Okell L, Aguas R, Boni MF.  
542 2022 Pre-existing partner-drug resistance to artemisinin combination therapies facilitates the

- 543 emergence and spread of artemisinin resistance: a consensus modelling study. *Lancet Microbe* **3**,  
544 e701–e710. (doi:10.1016/S2666-5247(22)00155-0)
- 545 43. Pongtavornpinyo W, Hastings IM, Dondorp A, White LJ, Maude RJ, Saralamba S, Day NP, White  
546 NJ, Boni MF. 2009 Probability of emergence of antimalarial resistance in different stages of the  
547 parasite life cycle. *Evol. Appl.* **2**, 52–61. (doi:10.1111/j.1752-4571.2008.00067.x)
- 548 44. Institut National de la Statistique et de la Démographie (INSD), Programme d’Appui au  
549 Développement Sanitaire (PADS), Programme National de Lutte contre le Paludisme (PNLP) et ICF.  
550 2018 Enquête sur les Indicateurs du Paludisme, 2017-2018. , 1–159.
- 551 45. Bennett ND *et al.* 2013 Characterising performance of environmental models. *Environ. Model. Softw.*  
552 **40**, 1–20. (doi:10.1016/j.envsoft.2012.09.011)
- 553 46. Filipe JAN, Riley EM, Drakeley CJ, Sutherland CJ, Ghani AC. 2007 Determination of the Processes  
554 Driving the Acquisition of Immunity to Malaria Using a Mathematical Transmission Model. *PLOS*  
555 *Comput. Biol.* **3**, e255. (doi:10.1371/journal.pcbi.0030255)
- 556 47. Ross A, Killeen G, Smith T. 2006 Relationships Between Host Infectivity to Mosquitoes and Asexual  
557 Parasite Density in Plasmodium Falciparum. *Am. J. Trop. Med. Hyg. Am J Trop Med Hyg* **75**, 32–37.  
558 (doi:10.4269/ajtmh.2006.75.32)
- 559 48. Hastings IM, Donnelly MJ. 2005 The impact of antimalarial drug resistance mutations on parasite  
560 fitness, and its implications for the evolution of resistance. *Drug Resist. Updat.* **8**, 43–50.  
561 (doi:10.1016/j.drug.2005.03.003)
- 562 49. Blasco B, Leroy D, Fidock DA. 2017 Antimalarial drug resistance: linking Plasmodium falciparum  
563 parasite biology to the clinic. *Nat. Med.* **23**, 917–928. (doi:10.1038/nm.4381)
- 564 50. President’s Malaria Initiative. 2019 Burkina Faso Malaria Operational Plan FY 2019. , 1–51.
- 565 51. Sondo P *et al.* 2020 Determinants of Plasmodium falciparum multiplicity of infection and genetic  
566 diversity in Burkina Faso. *Parasit. Vectors* **13**, 427. (doi:10.1186/s13071-020-04302-z)
- 567 52. Yekutieli P. 1960 Problems of epidemiology in malaria eradication. *Bull. World Health Organ.* **22**,  
568 669–683.
- 569 53. van der Pluijm RW *et al.* 2019 Determinants of dihydroartemisinin-piperaquine treatment failure in  
570 Plasmodium falciparum malaria in Cambodia, Thailand, and Vietnam: a prospective clinical,  
571 pharmacological, and genetic study. *Lancet Infect. Dis.* **19**, 952–961. (doi:10.1016/S1473-  
572 3099(19)30391-3)
- 573 54. Witkowski B *et al.* 2017 A surrogate marker of piperaquine-resistant Plasmodium falciparum  
574 malaria: a phenotype–genotype association study. *Lancet Infect. Dis.* **17**, 174–183.  
575 (doi:10.1016/S1473-3099(16)30415-7)
- 576 55. The RTS,S Clinical Trials Partnership. 2011 First Results of Phase 3 Trial of RTS,S/AS01 Malaria  
577 Vaccine in African Children. *N. Engl. J. Med.* **365**, 1863–1875. (doi:10.1056/NEJMoa1102287)

578 56. Datto MS *et al.* 2021 Efficacy of a low-dose candidate malaria vaccine, R21 in adjuvant Matrix-M,  
579 with seasonal administration to children in Burkina Faso: a randomised controlled trial. *The Lancet*  
580 **397**, 1809–1818. (doi:10.1016/S0140-6736(21)00943-0)

581

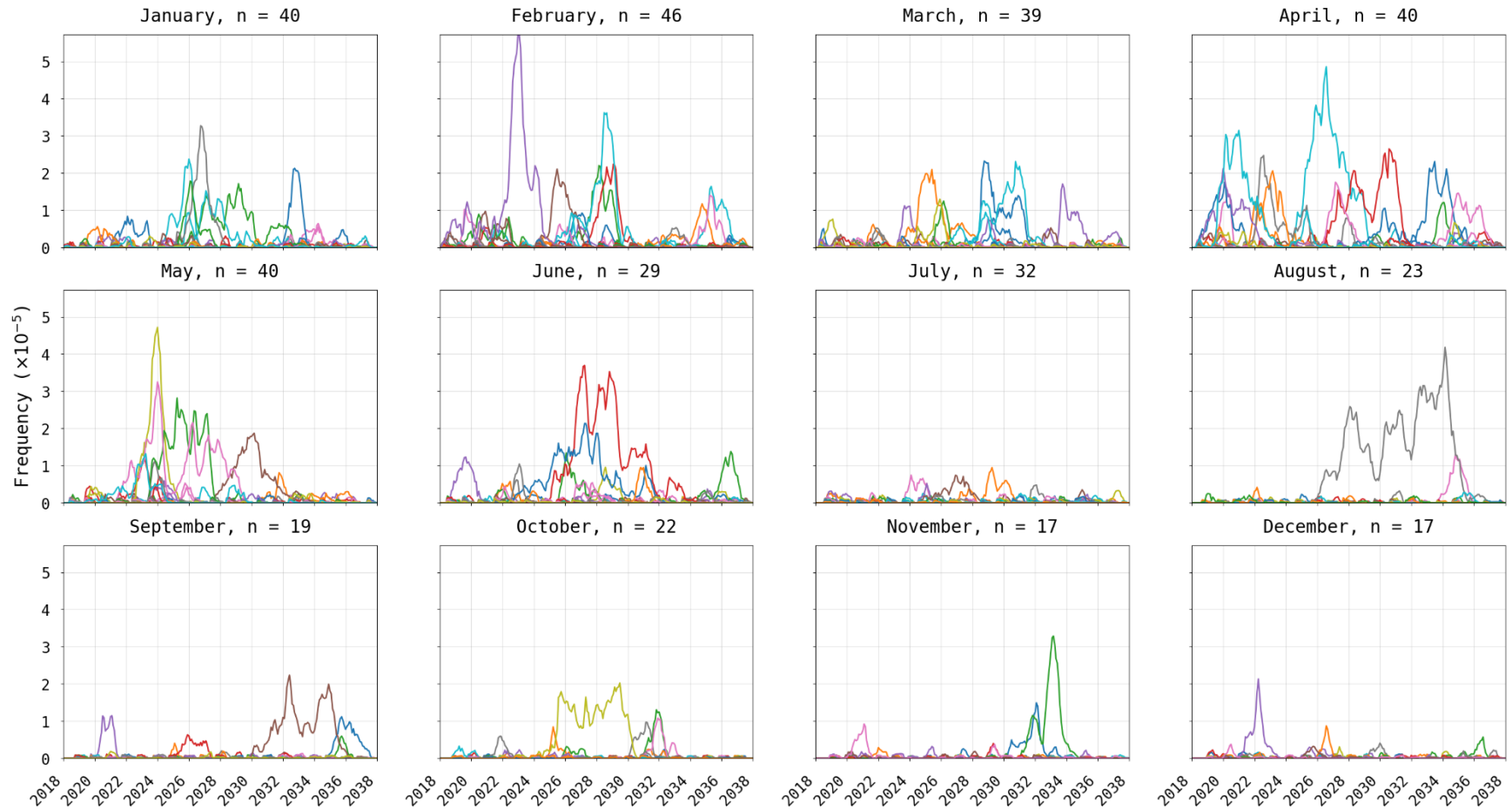
582 **Figure 1. 580Y frequency at model completion (after 20 years) based upon month of importation.**  
583 Circles show median allele frequency, bars show interquartile ranges, and violin plots show full range. As  
584 expected, the final frequency of 580Y increases as the number of importations increases (top to bottom)  
585 and when cases are symptomatic as opposed to asymptomatic (left to right). In most scenarios, importations  
586 that occur during periods of low seasonal transmission are more likely to result in establishment than cases  
587 imported during periods of high seasonal transmission (shaded region).



588

589

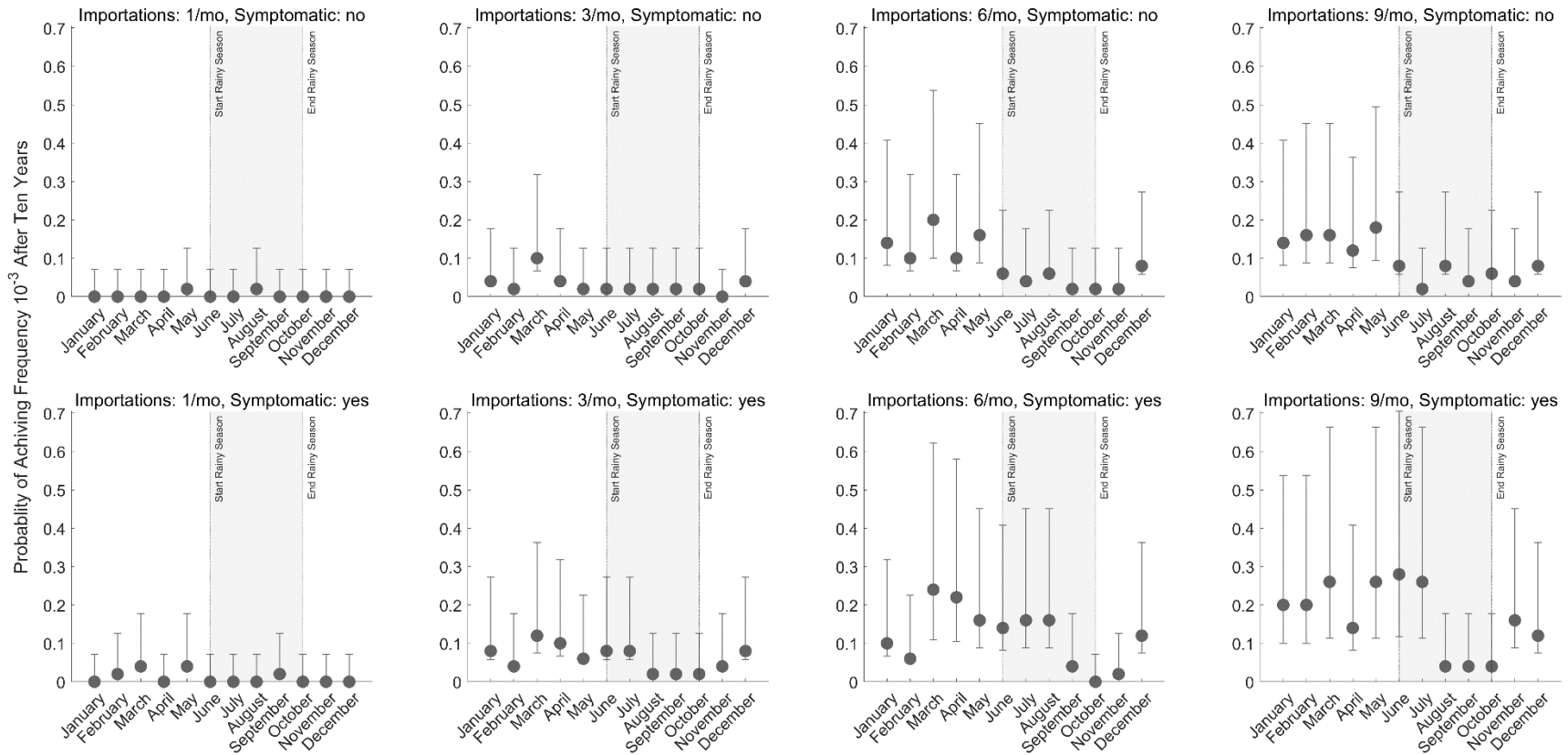
590 **Figure 2. Visualization of 580Y trajectories that reached extinction.** Plots show 580Y allele frequency trajectories under a scenario of one  
 591 asymptomatic importation per month and are broken up into twelve panels by month of introduction. Only trajectories that reached extinction, out  
 592 of fifty model runs, are shown. Title on each panel shows the month of introduction and the number ( $n$ ) of trajectories that reached extinction in the  
 593 first 20 years. The likelihood of extinction was higher in the low transmission season (78% to 92% during Jan-May) than in the high-transmission  
 594 season (34% to 64% during Jun-Dec).



595

596

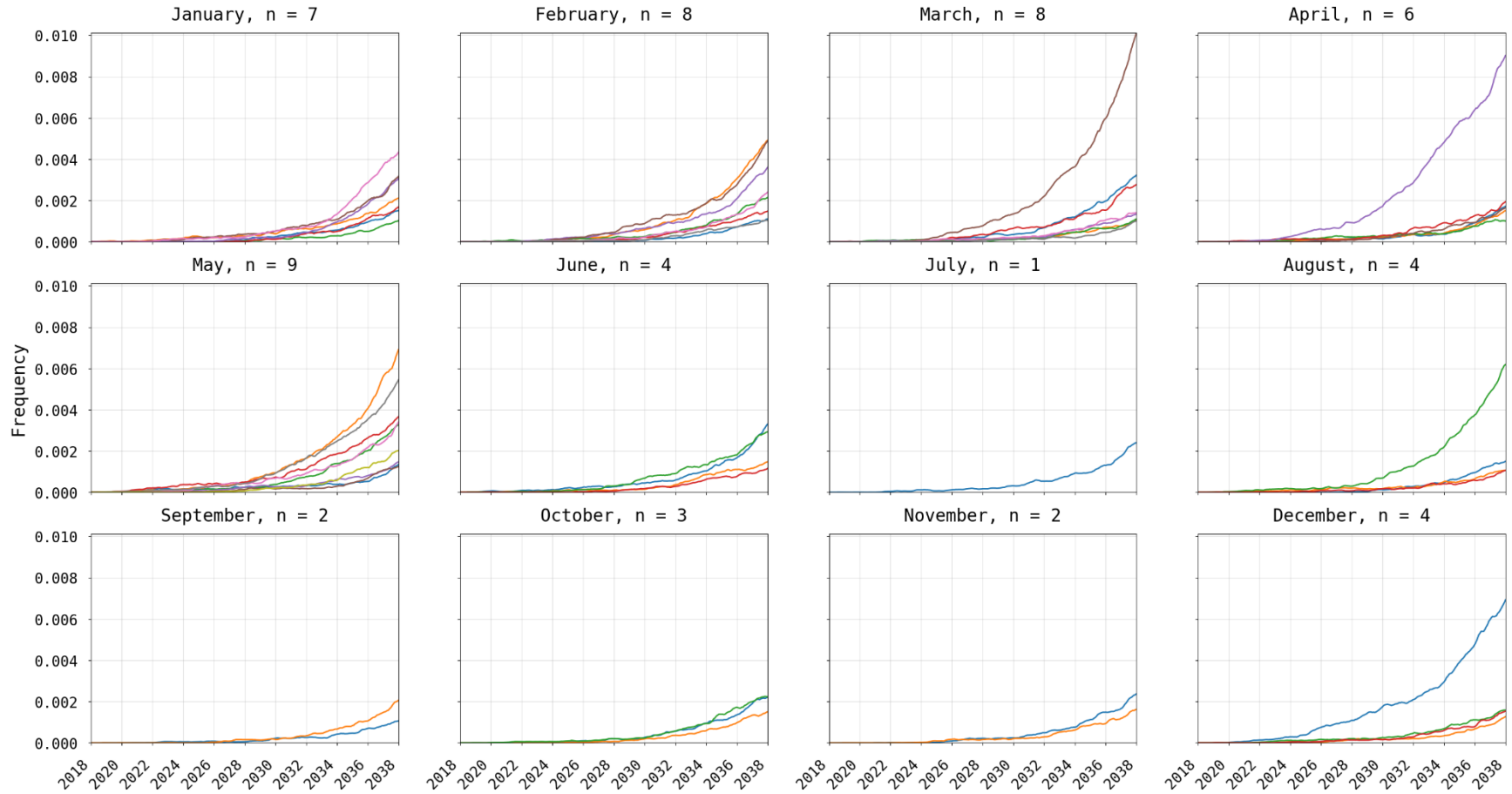
597 **Figure 3. Probability of successful emergence following importation.** Probabilities shown (circles) are maximum likelihood estimates from fifty  
 598 simulations and bars show 95% confidence intervals (exact binomial method). Probabilities of emergence are stratified by month of importation (x-  
 599 axis), by number of importation events per month (columns), and by whether the imported parasite occurred in an asymptomatic (top row) or  
 600 symptomatic (bottom row) individual. Successful emergence is generally more likely for parasites imported during low transmission season (non-  
 601 shaded).



602

603

604 **Figure 4. Visualization of 580Y trajectories that successfully emerged (frequency > 0.001).** Plots show 580Y allele frequency trajectories under  
 605 a scenario of nine asymptomatic importations per month and are broken up into twelve panels by month of introduction. Only trajectories that  
 606 reached an allele frequency >0.001, out of 50 simulations, are shown. Title on each panel shows the month of introduction and the number (*n*) of  
 607 trajectories that successfully emerged. Successful emergence was higher in the low transmission season (12% to 18% during Jan-May) than in the  
 608 high-transmission season (2% to 8% during Jun-Dec).

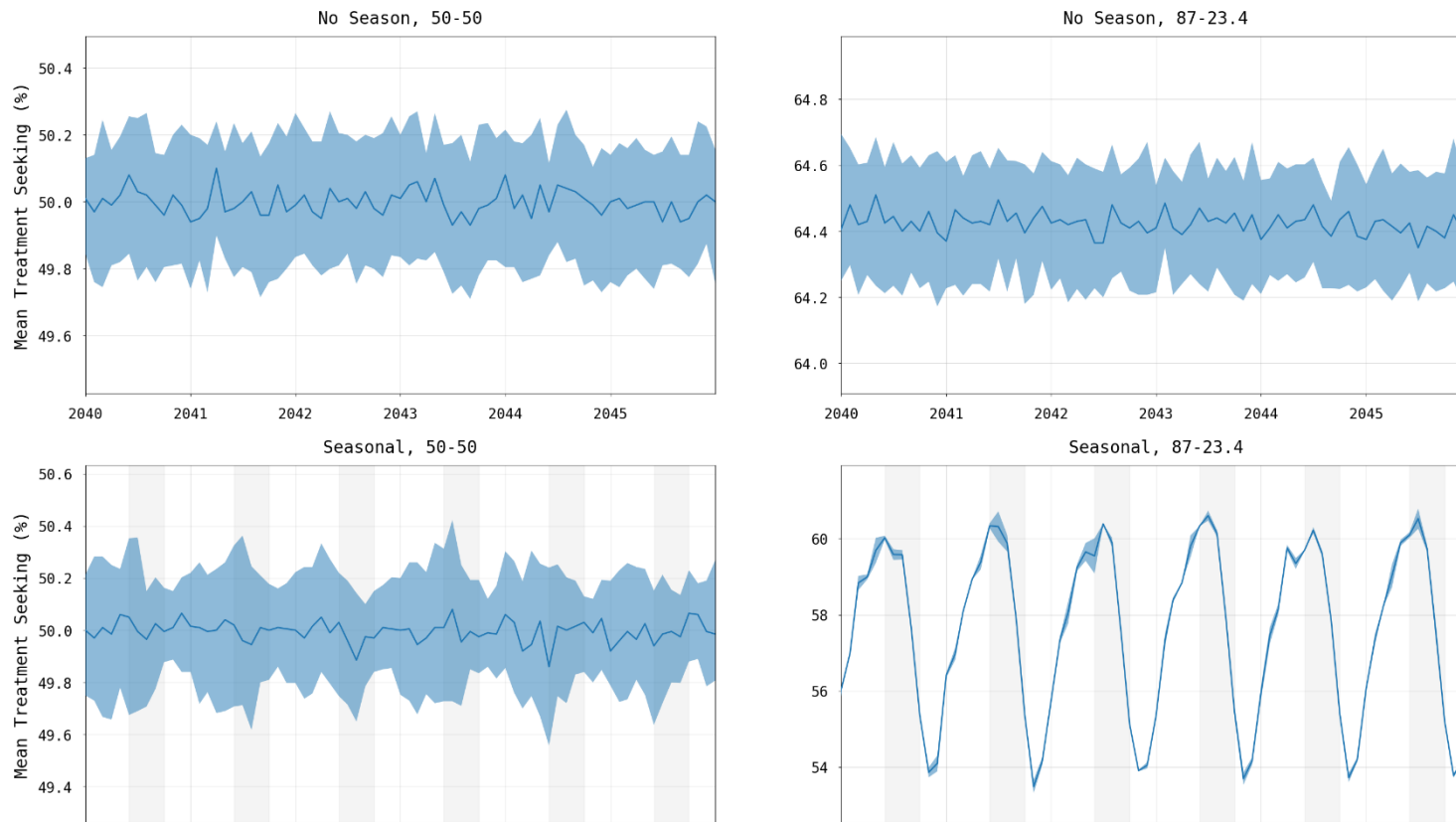


609

610



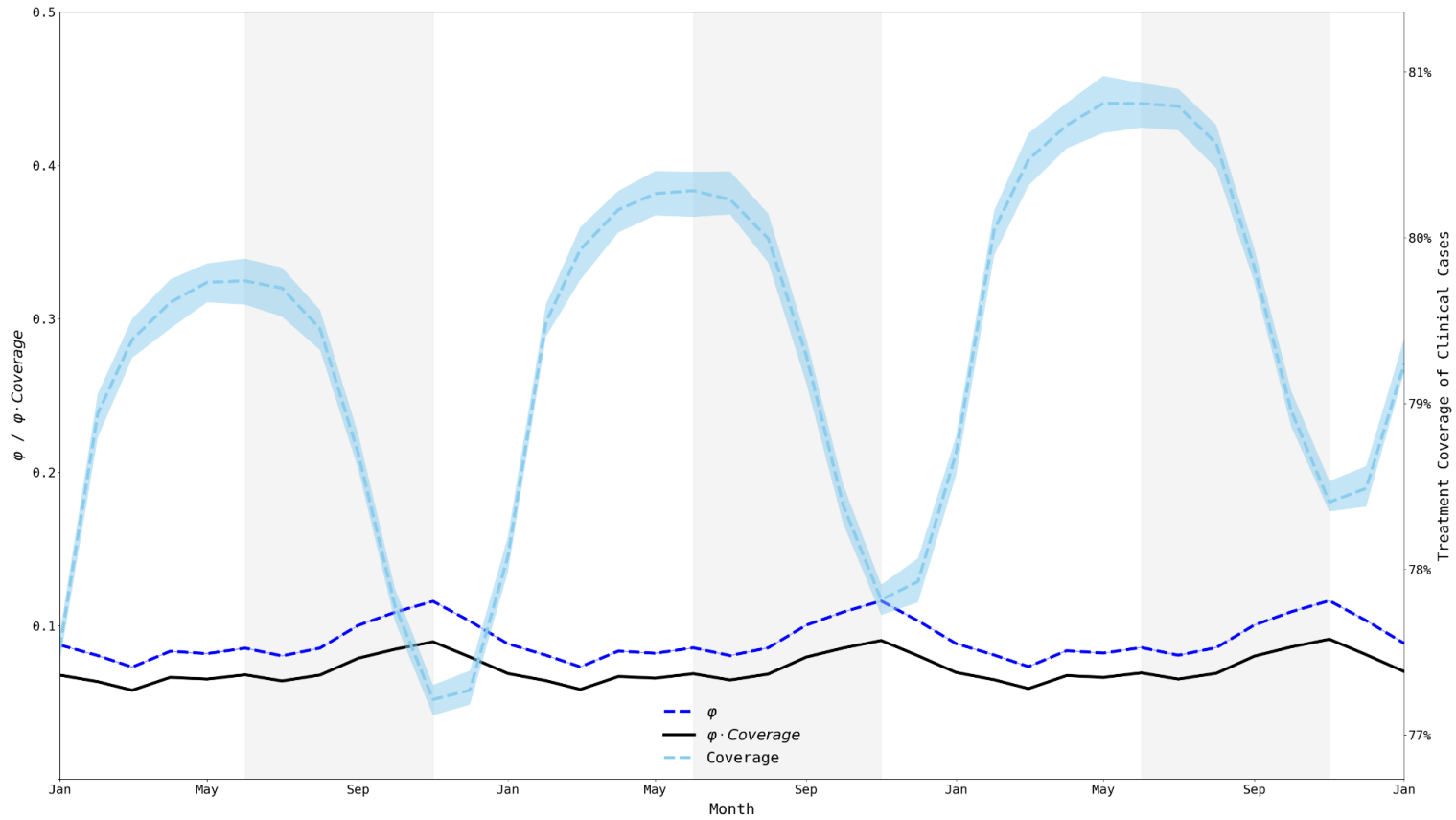
611 **Figure 5. Change in treatment seeking when controlling for seasonality and treatment seeking by age group.** Lines in each panel show  
612 median percentage of symptomatic malaria infections seeking treatment with shaded areas showing interquartile ranges from one hundred  
613 simulations. Panel titles show whether the epidemiological setting represents seasonal (right) or non-seasonal transmission (left), and whether  
614 treatment seeking is the same across age groups (“50-50”) with 50% of individuals seeking treatment (left) or uneven with 87% of children under-  
615 5 and 23.4% of individuals over-5 seeking treatment (right). In the presence of both seasonality and uneven treatment seeking across age groups,  
616 treatment coverage and thus selection pressure change through time (bottom right).



617

618

619 **Figure 6. Treatment coverage and fraction symptomatic ( $\phi$ ) from Jan 1, 2033, to Jan 1, 2036.** When examining a 36-month window, we  
 620 clearly see that the population treatment coverage is slowly increasing (consistent with a gradual increase in treatment seeking over time) and that  
 621 treatment coverage (right-axis) fluctuates moderately with the transmission season. The fraction of all infections that are symptomatic ( $\phi$ ) remains  
 622 relatively constant (between 0.073 and 0.117) but fluctuates out-of-phase with treatment coverage. The product of  $\phi$  and coverage (black line)  
 623 fluctuates between 0.058 and 0.092. Medians and IQRs (shaded areas) shown from fifty simulations.

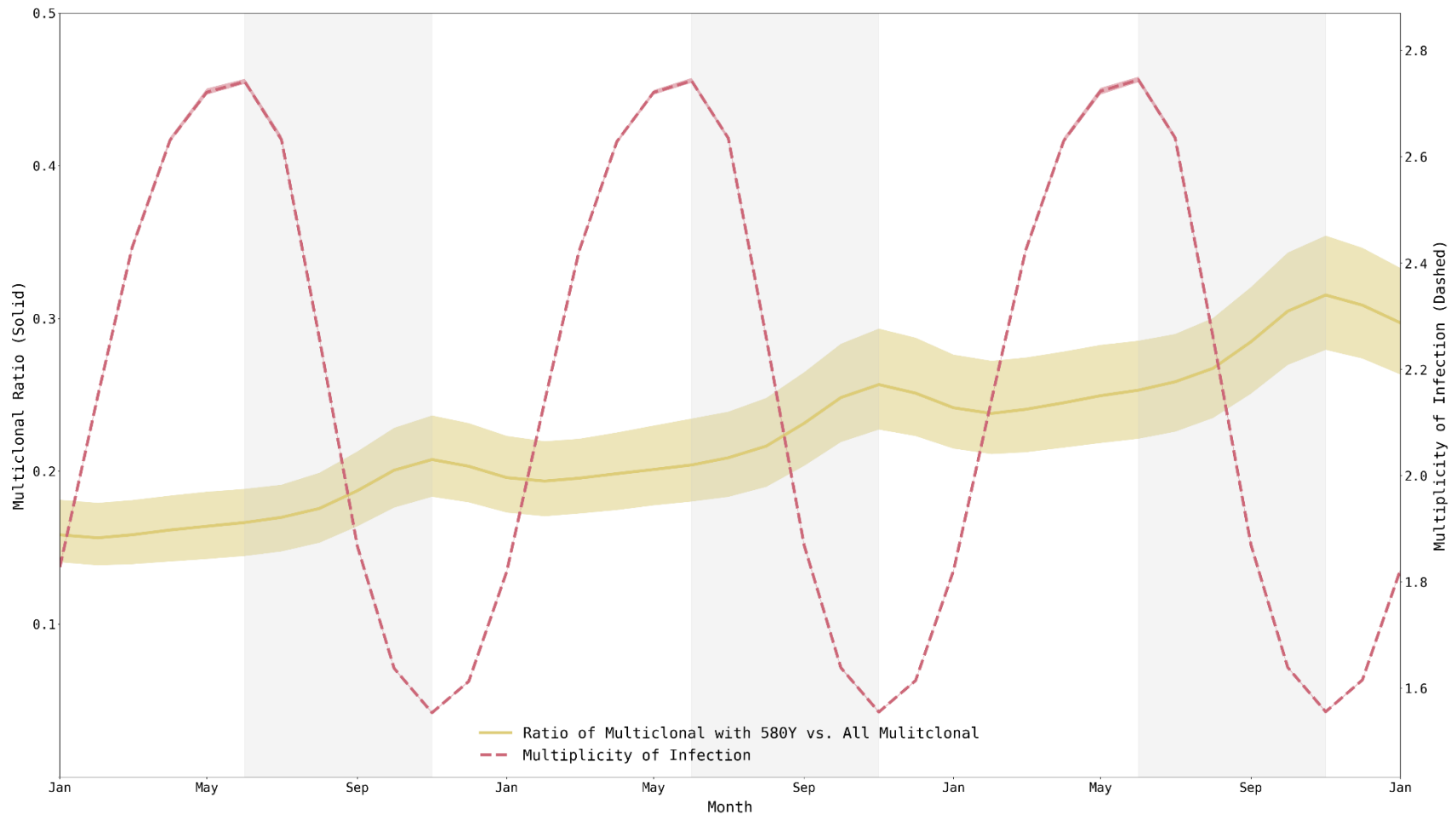


624

625

626 **Figure 7. Multiplicity of infection and fraction of multi-clonal infections harboring resistant alleles, from Jan 1, 2033, to Jan 1, 2036.** Mean  
 627 multiplicity of infection (MOI) across individuals ranges from 1.55 to 2.75, peaking at the end of the low-transmission season. Fraction of  
 628 multiclonal infections that harbor resistant alleles also fluctuates and peaks at the end of the high-transmission season (out of phase with MOI).  
 629 There does not appear to be a particular period when 580Y alleles are experiencing maximum within-host competition from wild-type parasites.  
 630 Medians and IQRs (shaded areas) shown from fifty simulations.

631



632